Penerbit Akademia Baru

Journal of Advanced Research Design

Journal homepage:
https://akademiabaru.com/submit/index.php/ard
ISSN: 2289-7984

The Influence of Deposition Time on Zinc oxide-based Nanostructures by Microwave-assisted Sonochemical Technique

Nurfatini Atiqrah Khairul Azhar[1,2], Mohd Firdaus Malek[1,2*], Kevin Alvin Eswar[1,2,3], Maryam Mohammad[1,2,4], Nur Fairuz Rostan[1,2], Zahidah Othman[1,2], Nurul Zulaikha Mohammad Zamri[1,2], Muhamad Kamil Yaakob[1,2], Asiah Mohd Nor[1,2], Ruziana Mohamed[1,2], Tetsuo Soga[5]

[1] NANO-SciTech Lab (NST), Centre for Functional Materials and Nanotechnology (CFMN), Institute of Science (IOS), Universiti Teknologi MARA (UiTM), 40450 Shah Alam, Selangor, Malaysia
[2] Faculty of Applied Sciences, Universiti Teknologi MARA (UiTM), 40450 Shah Alam, Selangor, Malaysia
[3] Department of Physics, Faculty of Applied Sciences, Universiti Teknologi MARA (UiTM), Sabah Branch, Tawau Campus, 91000 Sabah, Malaysia
[4] Department of Physics, Faculty of Applied Sciences, Universiti Teknologi MARA (UiTM), Perak Branch, Tapah Campus, Tapah Road, 35400 Perak, Malaysia
[5] Department of Electrical and Mechanical Engineering, Nagoya Institute of Technology (NITech), Showa-ku, Gokiso-cho, Nagoya, 466-8555, Japan

ARTICLE INFO

Article history:
Received 10 February 2026
Received in revised form 30 May 2026
Accepted 2 June 2026
Available online 14 August 2026

Keywords:
Dip coating; Microwave; PET; Time; Zinc oxide Nanostructures

ABSTRACT

Zinc oxide (ZnO) nanostructures have attracted significant attention due to their biocompatibility and versatile applications in electronics, optoelectronics, photocatalysis and sensing. The Sustainable Development Goals emphasise the need for advanced, environmentally friendly nanomaterials, where microwave-assisted sonochemical synthesis offers a rapid and uniform approach to producing high-quality ZnO nanostructures. However, the effect of deposition time on the properties of ZnO nanostructures synthesised via microwave-assisted sonochemical methods remains inadequately understood. Existing studies have not comprehensively explored how this critical parameter influences crystallinity, morphology and optical behavior, especially when it comes to real life applications. This study addresses this gap by systematically investigating the impact of deposition time to optimise ZnO nanostructures quality for sustainable nanotechnology applications. This paper presents an investigation on the influence of deposition time on zinc oxide-based nanostructures by using microwave-assisted sonochemical technique. Zinc oxide nanostructures (Zn-Ns) were synthesised by preparing the seed layer using ultrasonic-assisted dip-coating technique on both sides of polyethylene terephthalate (PET) as substrate. The Zn-Ns growth was precisely controlled by adjusting the deposition times varying from 30, 60, 90, 120 and 150 minutes. The structural, morphological and optical properties of each sample were characterized by using X-ray Diffraction (XRD), Field Emission Scanning Electron Microscopy (FESEM) and Ultraviolet-Visible (UV-Vis) Spectroscopy. Results revealed that there is a dominant peak on XRD analysis that is believed to be the (200) cubic phase zinc oxide and different surface morphologies were also observed for FESEM images as the deposition time varies. Meanwhile, the UV-Vis spectroscopy portrayed a decrease in trend when the deposition time increased from 30 minutes to 150 minutes due to the transmittance of thin films decreasing as film thickness increases. A nanogenerator has been fabricated and an output voltage of near 8V has been obtained, proving a successful application of this study. Thus, this work suggested a new approach on the synthesisation of Zn-Ns by using microwave-assisted sonochemical technique which

* *Corresponding author*
E-mail address: mfmalek07@uitm.edu.my; mfmalek07@gmail.com

resulted in many potentials for future applications such as nanogenerators, dye-sensitized solar cell (DSSC) and sensors.

1. Introduction

Sustainable Development Goals is a framework provided by United Nation to urge a transformative era of scientific and technological advancements, without jeopardising the life and nature of our own in order to achieve these life-changing goals by 2030. These goals offers unparalleled opportunities for nanotechnology and especially zinc oxide (ZnO), as a biosafe and biocompatible inorganic material [1]. Zinc oxide offers manifold structures such as nanodisks [2], nanosheets[3] and nanorods[4]. Zinc oxide can be categorised by four different groups based on their dimensions namely zero dimensional (0-D), one dimensional (1-D), two dimensional (2-D), and three dimensional (3-D). Besides, unique and versatile property that is possessed by zinc oxide such as a direct wide bandgap of 3.37 eV [5] have found applications in miscellaneous fields, such as electronics [6, 7], optoelectronics [8, 9] , photocatalysis [10-12] and sensing [13, 14]. The purpose of the present study is to systematically investigate how deposition time impacts the structural, morphological and optical properties of ZnO nanostructures synthesised via the microwave-assisted sonochemical technique. In the pursuit to harness the full potential of zinc oxide nanostructures, many studies have introduced numerous synthesis techniques to precisely control the size, shape and crystallinity [15]. One particularly promising approach is the utilisation of microwave-assisted sonochemical techniques [16]. This innovative methodology is a combination of microwave irradiation with ultrasonic cavitation, offering several advantages, including rapid synthesis, enhanced reaction rates, and the ability to produce highly uniform nanoparticles [17]. The deposition time during the synthesis process has emerged as a critical parameter that significantly influences the properties of zinc oxide nanostructures. Several studies have highlighted the importance of deposition time in determining particle size, crystallinity and morphology [18, 19].

Besides, many recent findings suggest that microwave heating is energy efficient and can achieve high crystalline zinc oxide in a much shorter time compared to conventional heating techniques that rely on convection [20]. This extended duration can result in undesirable consequences such as thermal gradients within the bulk medium and less effective and non-uniform reactions, which, in turn, impede the growth of crystals. Despite numerous existing studies on ZnO nanostructures synthesised by various methods, understanding of deposition time effects within microwave-assisted sonochemical synthesis remains limited. Although earlier research has explored the roles of deposition time in ZnO growth, none have comprehensively assessed these effects under the synergistic microwave-ultrasound environment, which combines rapid microwave heating and ultrasonic cavitation to achieve enhanced reaction kinetics, uniform nucleation, and shortened synthesis duration. Conventional heating techniques often suffer from extended reaction times causing thermal gradients, less uniform crystallisation, and detrimental effects on nanostructure quality. This research fills this critical gap by providing an in-depth, systematic analysis of time-dependent growth characteristics specific to microwave-assisted sonochemical processes. The novelty of this study lies in its unique exploration of the microwave-assisted sonochemical technique,

a hybrid approach that leverages the advantages of microwave irradiation and ultrasonic cavitation to finely tune ZnO nanostructure properties through precise control over deposition time. Unlike previous studies focusing on conventional or single-mode synthesis methods [21, 22], this research demonstrates how optimising deposition time can directly influence crystallinity, morphology and optoelectronic attributes, thereby enabling tailored ZnO nanostructures for diverse applications. This work is important because it contributes to both fundamental understanding and practical synthesis of ZnO nanostructures with enhanced performance, directly supporting sustainable nanotechnological advancements aligned with the SDGs. Therefore, this study elucidates the influence of deposition time on the evolution of ZnO nanostructures within the microwave-assisted sonochemical framework, offering critical insights for researchers and industry practitioners to design more efficient, rapid and environmentally sustainable synthesis protocols that support the advancement of ZnO nanomaterials in high-impact technological applications.

2. Materials and Methods

2.1 Materials

Zinc Acetate Dihydrate [$Zn(CH_3CO_2)_2{\cdot}2H_2O$], Monoethanolamine [MEA (C_2H_7NO)], Ethanol (CH_3CH_2OH), Zinc Nitrate Hexahydrate [$Zn(NO_3)_2.6H_2O$], Hexamethylenetetramine [HMTA ($C_6H_{12}N_4$)] and Deionised Water (DI Water).

2.2 Zinc oxide seeded layer preparation

The preparation of zinc oxide seed layer first starts with the cleaning of flexible polyethylene terephthalate (PET) of a size of 2cm x 2cm as the substrate. The PET were cleaned with ethanol and DI water for 10 minutes each in an ultrasonic bath and then were left to dry in the air to remove the moisture. Ultrasonic-assisted dip-coating technique was used to coat the PET on both sides. The seed solution was prepared beforehand by dissolving zinc acetate dehydrate [$Zn(CH_3CO_2)_2{\cdot}2H_2O$] in ethanol to obtain the concentration of 0.4 mol/L. Monoethanolamine, [MEA (C2H7NO)] which acts as stabiliser was then added and the MEA:zinc acetate molar ratio was kept constant at 1:1 [23]. The solution was stirred to obtain a uniform and clear solution. Next, after attaching the substrate to the dip-coater, the substrates were dipped into the solution for 10 seconds with both upward and downward speed of 40 mm/s to obtain a uniform distributed seed layer across the PET. This process was repeated five times with an interval of a heating process of 100°C for 10 minutes after each dip. The heating process was done to eliminate the solvent residue and ensure strong adhesion of the seed layer. Finally, the zinc oxide seed layer was heated to 100°C for 25 minutes to improve the crystalline quality.

2.3 Growth of zinc oxide nanostructures

Next, an aqueous solution of 12.5 mM zinc nitrate hexahydrate [$Zn(NO_3)_2.6H_2O$] and hexamethylenetetramine [HMTA, $C_6H_{12}N_4$] were mixed with 1000ml of DI water. The solution was stirred for 30 minutes to achieve homogeneous solution. Subsequently, the solution underwent ultrasonic treatment within a water bath at a temperature of 50°C for a duration of 30 minutes, employing a 40 kHz frequency (Hwasin Technology Powersonic 405). The solution later was allowed to age for 1 hour at room temperature. After that, the solution was given another 1 hour of stirring without adding any heat. Later, the solution was transferred into a 100ml Scott bottle and the zinc

oxide seed layer was submerged into the growing solution. The microwave was set to 200-watt power for various deposition times (30, 60, 90, 120 and 150 minutes). Lastly, the substrate was removed from the solution, washed with DI water to remove the residues on the surface and left to dry in air.

2.4 Fabrication of ZnO nanogenerator

The ZnO nanogenerator was fabricated by placing a layer of battery-grade aluminum foil on top of the PET substrate. The aluminum foil acted as the top electrode, while the PET served as the bottom electrode. Kapton tape was used to hold the layers together and ensure stable contact during testing.

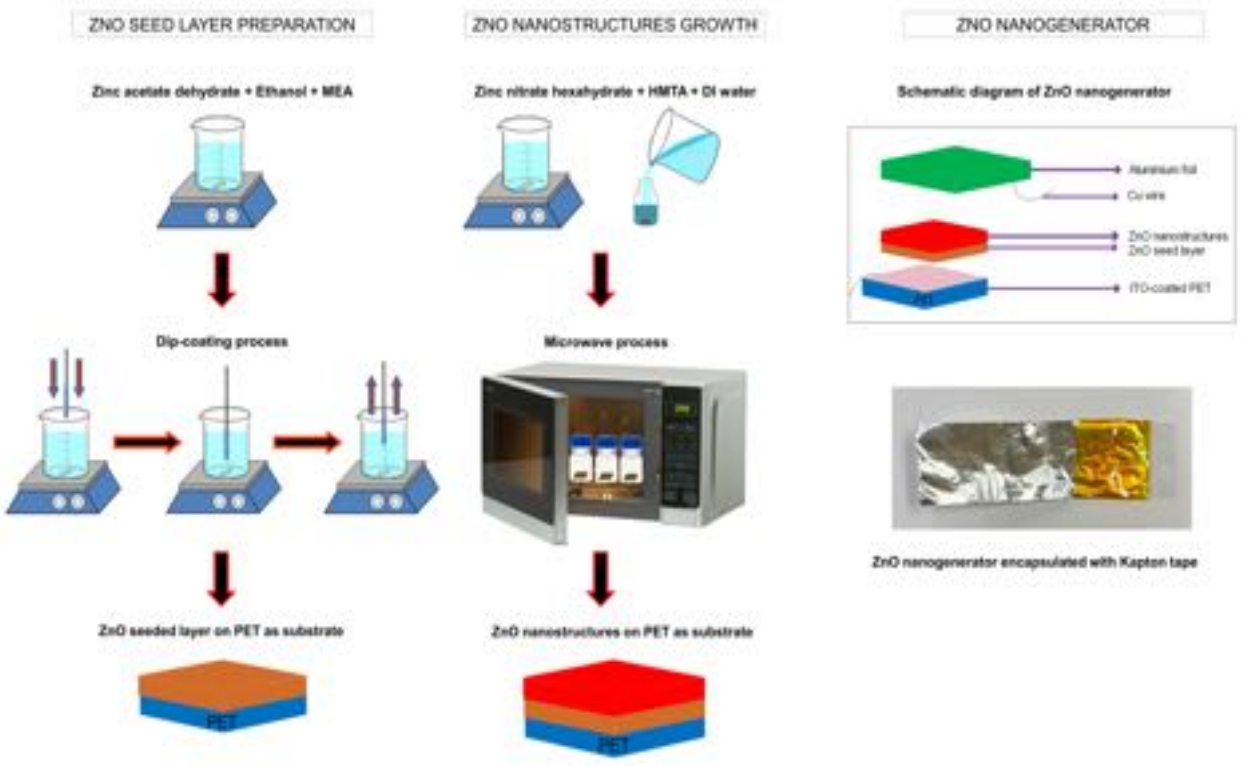

Figure 1. The schematic diagram of methodology conducted.

2.5 Characterisation of Zinc oxide nanostructures

The structural properties of zinc oxide nanostructures were analysed by using X-ray diffraction (XRD, PANalytical X'Pert3 PRO) at 45 kV and 40 mA with Cu-Ka radiation at ca. 2θ = 5°-90°. The average crystallite size, D of the zinc oxide nanostructures deposited at various growth time was calculated by using Scherrer's formula shown in Eq. (1):

$$D_{(hkl)} = \frac{k\lambda}{\beta_{(hkl)} \cos\theta} \qquad (1)$$

Where k is a constant shape approximately equal to 0.94 for spherical crystallites, λ = 1.5406 Å represents the wavelength of the incident X-rays and β is the full width broadening at half maximum (FWHM).

The surface morphology of the structure of all samples was characterised by field emission scanning electron microscopy (FESEM, Analytical High Resolution Field Emission Scanning Electron Microscope Apreo 2S (Thermo Fischer Scientific). The optical properties were characterised by using UV-Visible Spectroscopy (UV-Vis, Cary 5000). The nanogenerator performance was characterised by using oscilloscope (Keithley 2420 Sourcemeter).

3. Result and Discussion

Figure 2 shows the X-ray diffraction (XRD) pattern of zinc oxide nanostructures (Zn-Ns) grown under different deposition times (30, 60, 90, 120 and 150 min) using microwave-assisted sonochemical method. The peaks of zinc oxide and polyethylene terephthalate (PET) were observed in all samples. PET peaks at ~44.5° were dominant in all the samples, indicating that zinc oxide did not have uniform distribution on the substrate. Zinc oxide crystallises in two main forms, hexagonal wurtzite and cubic zincblende. It was observed that (200) peak of zinc oxide at ~38.4° is indexed to cubic crystal system (JCPDS card no. 03-065-2880) [24] meanwhile all the other (100), (002) and (101) peaks are indexed to hexagonal crystal system (JCPDS card no. 01-079-0205) [25]. There was none hexagonal crystal system peak obtained in sample that underwent 30 min of deposition time, but as the deposition time increases to 60 min, it can be seen that (100) peak at ~31.9° and (101) peak at ~36.4° started to emerge. However, the (002) peak at ~34.6° can only be seen at sample that underwent 90 min of deposition time and above. The sample at 30 minutes, although the shortest deposition time, showed a strong and sharp (200) peak, indicating a preferential orientation in the cubic crystal system. This dominant (200) peak correlates well with the nanoflake morphology observed later in the FESEM image for this sample, suggesting that early-stage growth under this synthesis condition favours lateral expansion and flat surface development. The presence of highly oriented (200) planes implies a specific crystallographic growth along the [200] direction, which may provide enhanced surface area and more active sites for interfacial interaction, potentially benefiting piezoelectric and sensor applications. Unlike the commonly preferred (002) peak from the hexagonal system that reflects vertical alignment along the c-axis, the (200)-oriented growth offers a unique structural arrangement, nanoflakes lying relatively flat and interconnected, likely improving mechanical flexibility and electron mobility across the plane [26].

Besides, this XRD analysis also suggests that both cubic crystal system and hexagonal crystal system co-exist after 60 minutes of deposition time. The XRD analysis of ZnO nanostructures synthesised at different deposition times (30, 60, 90, 120, and 150 minutes) reveals a clear transition from a metastable cubic phase to a thermodynamically stable hexagonal wurtzite structure as the reaction time increases as shown in figure 2. At 30 minutes, the pattern is dominated by a sharp peak at approximately 38.4°, attributed to the (200) plane of cubic zincblende ZnO (JCPDS No. 03-065-2880). The absence of hexagonal peaks such as (100), (002), and (101) suggests that the material initially crystallizes in the cubic phase, likely due to rapid supersaturation and non-equilibrium conditions induced by microwave-assisted synthesis [27]. Early-stage cubic phase stabilisation under microwave or solvothermal conditions has been observed in other studies, particularly on non-crystalline or mismatched substrates, where surface energy and reaction kinetics strongly influence phase selection. Next, at 60 minutes of deposition time, new diffraction peaks corresponding to the hexagonal wurtzite structure begin to appear, specifically (100) and (101), while the (200) cubic peak remains prominent. This suggests an intermediate phase regime, where the ZnO begins to transition structurally but remains compositionally mixed. By 90 minutes, all three major hexagonal peaks, which are (100), (002), and (101) are evident, indicating that the hexagonal phase is now substantially present. However, the (002) peak intensity remains relatively weak compared to the other hexagonal

reflections, implying limited preferential orientation along the c-axis. At 120 minutes of deposition time, the (002) peak intensifies significantly, while the (200) cubic peak diminishes, indicating enhanced c-axis alignment and a transition toward a wurtzite-dominant phase. The sequential comparison of Figures 2(a), 2(c), and 2(d) thus reveals a time-driven crystallographic evolution. Initially, the cubic phase dominates, followed by a phase coexistence regime at 90 minutes, and finally a near-complete transformation into hexagonal wurtzite at 120 minutes. The comparison between Figures 2(a), 2(c), and 2(b) further clarifies the transition process, the 60-minute sample acts as a structural bridge between the purely cubic state and the mixed-phase configuration. Such gradual transitions have been observed in solution-based and microwave-assisted ZnO syntheses, where sufficient energy input and time are required to overcome kinetic barriers and allow structural reorganisation of Zn–O tetrahedra into the wurtzite lattice.

Moreover, this result proposes that the zinc oxide nanostructures did not grow perpendicularly to the substrate, due to (002) peaks obtained were relatively small compared to other peaks. The absence of a dominant (002) reflection implies that preferential c-axis (vertical) growth was suppressed, while lateral crystallographic orientations, particularly the (200) plane were favoured. This growth behaviour is consistent with the development of nanostructures in a planar or oblique alignment with respect to the substrate surface, correlating with the observed nanoflake morphology. In this context, perpendicular to the substrate refers to vertical alignment of ZnO crystallites along the [002] direction, which is typically associated with the formation of vertically aligned nanorods or nanowires. Such vertical orientation is generally advantageous in piezoelectric and optoelectronic applications due to enhanced charge transport and separation along the c-axis [28]. However, in the present study, the dominant (200) orientation and resulting nanoflake structures may offer increased surface contact area and mechanical flexibility, characteristics that are beneficial for flexible nanogenerator applications [29].

However, among all the tested samples, the 30-minute deposition with dominant (200) orientation is considered most favourable from a crystallographic standpoint for nanogenerator application. The XRD pattern revealed a strong and sharp (200) diffraction peak, indicating a preferential orientation within the cubic phase of ZnO. In contrast to the (002) orientation which corresponds to vertical alignment along the c-axis and is often associated with hexagonal wurtzite structures [30], the (200) plane suggests that the crystallites are aligned laterally or obliquely relative to the substrate surface. This orientation may facilitate better integration with flexible substrates, promoting more effective mechanical coupling and stress distribution during operation. As such, the dominance of the (200) peak under optimized deposition conditions suggests a favourable crystallographic alignment for flexible piezoelectric applications. This highlights the importance of tailoring the crystal orientation through precise control of deposition parameters to achieve desired structural characteristics aligned with specific device requirements.

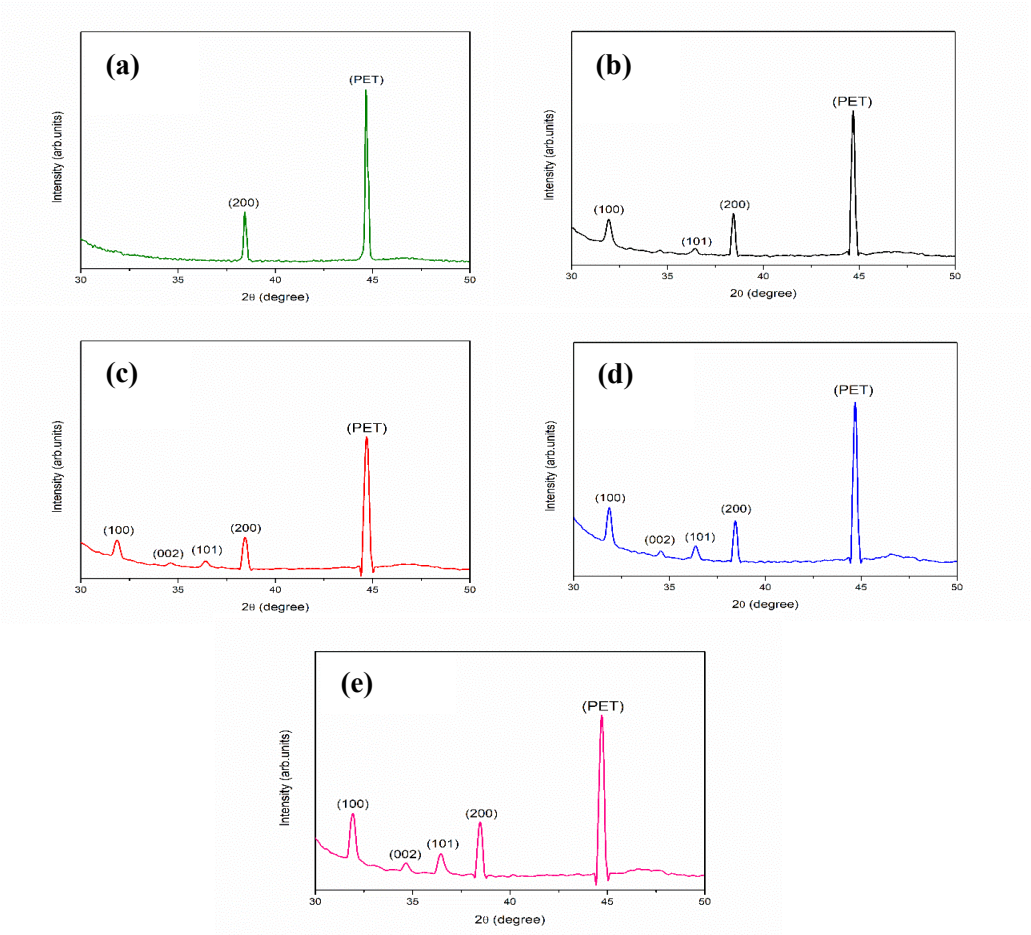

Figure 2. The XRD patterns of zinc oxide nanostructures grown at various growth time a) 30 b) 60 c) 90 d)120 and e) 150 min.

The average crystallite size for each sample were measured using the above equation (1) and the obtained values for 30, 60, 90, 120 and 150 min are 51.46, 33.85, 28.75, 34.89 and 28.94 nm, respectively. The average crystallite sizes of zinc oxide nanostructures show a decrease trend as the deposition time increases up until 120 min where the crystallite size increases before it declined again at 150 min of deposition time. A steady decrease in crystallite sizes up to 90 minutes suggests high nucleation density and lattice strain during phase transition. The increase at 120 minutes corresponds to oriented growth and grain enlargement as the hexagonal phase dominates [31]. A final decrease at 150 minutes may reflect growth saturation or limited nutrient availability. Concurrently, Figure 3 illustrates that the intensities of the (002), (100), and (101) hexagonal peaks increase with time, while the cubic (200) peak diminishes, further affirming the transformation from metastable to stable phase. This phase and orientation control is crucial in tuning ZnO's functional properties, especially for optoelectronic, piezoelectric, and sensing applications [32].

Figure 3 shows the intensities of each peak and diffraction angles of zinc oxide nanostructures prepared at various growth times. There is minimal variation in the diffraction angles across all samples for the characteristic ZnO peaks, indicating that no significant peak shifting or formation of secondary phases occurred. There is not much difference between the diffraction angles on all the graphs for all peaks of zinc oxide, indicating that they are all relatively pure. This consistency suggests that the ZnO nanostructures are all relatively pure, as the positions of the diffraction peaks remain in good agreement with standard JCPDS reference patterns and show no evidence of lattice

distortion, impurity incorporation or structural transformation. The diffraction angle (2θ) and intensity evolution of ZnO nanostructures as a function of deposition time from 30 to 150 minutes provides critical insights into crystal orientation, lattice strain behaviour and phase transformation. Figure 3 illustrates the relationship between growth time and the diffraction features for the (100), (002), (101), and (200) planes corresponding to both hexagonal wurtzite and cubic phases of ZnO. Specifically, Figures 3 (a–c) represent the hexagonal phase reflections, while Figure 3 (d) corresponds to the (200) reflection of the cubic phase. The systematic trends in both angle and intensity underscore a dynamic reorganisation of the ZnO lattice during microwave-assisted sonochemical deposition. In Figures 3 (a–c), the (100), (002), and (101) peaks show noticeable fluctuations in 2θ values over time. For instance, the (002) peak [Figure 3 (b)] displays a significant shift from ~34.5° to higher values between 60 and 90 minutes, indicating lattice contraction along the c-axis. This may be attributed to increasing internal stresses due to anisotropic vertical growth as nanostructures begin to orient preferentially along the c-axis. Similarly, minor shifts in (100) and (101) diffraction angles also imply adjustments in lattice parameters, possibly due to stress relaxation, rearrangement of surface atoms and densification of the wurtzite structure. In contrast, the (200) peak in Figure 3(d), associated with the cubic ZnO phase, shows relatively stable diffraction angles over time. This stability suggests minimal structural evolution in the cubic phase compared to the dynamic lattice reorientation occurring within the hexagonal domains. The contrast between the stable cubic (200) and fluctuating hexagonal peaks supports the conclusion that the hexagonal phase is actively growing and reorganising, while the cubic phase is gradually being phased out without significant lattice distortion. This comparative behaviour confirms that diffraction angle shifts are an important indicator of phase-specific structural transitions and strain effects during ZnO growth.

Next, peak intensity in XRD is indicative of the relative degree of crystallinity, preferred orientation (texture) and population of crystallites aligned along a specific lattice plane [33]. The intensity, however, shows an upward trend for peak (002) and (101) as the deposition time increases. Figure 3 (a) observed that as the deposition time increases from 60 min to 90 min, there is a decrease in intensity which then continue to portray a constant surge as the deposition time increases till 150 min for peak (100). This might be due to the presence of (002) peak on the 90 min sample. The increasing trend in all these three peaks demonstrates that the samples slowly grow into the hexagonal crystal structure as proposed by the XRD pattern mentioned earlier. Meanwhile, figure 3 (d) shows an obvious slump in intensity as the deposition time increases. This proves that the cubic crystal system steadily decreases as the samples exhibit both hexagonal and cubic crystal system in the latter samples.

The time-resolved intensity variations in Figures 3 (a–c) reflect the progressive crystallisation and orientation evolution of the hexagonal ZnO structure. The (100) peak [Figure 3 (a)] shows a moderate rise in intensity from 60 to 150 minutes, indicating enhanced grain alignment in the lateral a-direction. The trend suggests that while the (100) orientation becomes more prominent over time, it does so gradually, potentially reflecting lateral crystal fusion or nanostructures sidewall thickening. The (002) peak [Figure 3 (b)] exhibits the most dramatic increase in intensity from 60 to 90 minutes, followed by stabilisation. This behaviour is emblematic of the rapid development of c-axis aligned nanorods or nanowires, a hallmark of ZnO grown under directional energy inputs such as microwave or hydrothermal conditions. This intense growth along the vertical axis is energetically favoured due to the lower surface energy of the (002) plane and results in columnar nanostructures with higher aspect ratios. In parallel, the (101) peak [Figure 3 (c)] continues to increase steadily across all time intervals, albeit at a more modest rate. This may be attributed to general crystal growth and coalescence in off-axis directions. The persistence of this orientation alongside (002) and (100)

suggests a polycrystalline nature with multiple orientation domains that evolve over time. Conversely, the (200) peak intensity in Figure 3 (d) steadily declines from 30 to 120 minutes, corresponding to the reduction of the metastable cubic phase. The initial high intensity at 30 minutes can be attributed to rapid nucleation of cubic ZnO under high supersaturation during early deposition. However, this phase is thermodynamically less stable than the hexagonal counterpart, and over time, it diminishes as hexagonal crystallites grow and reorient, overtaking the phase landscape. Overall, the peak intensity variations across all orientations can be attributed to a combination of nucleation kinetics, crystal growth mechanisms and surface energy minimisation. Early stages favour high nucleation rates and random orientations, while extended deposition time promotes thermodynamic reordering, grain coarsening and orientation alignment, particularly along the c-axis. The cubic-to-hexagonal phase transformation and the corresponding intensity evolution reveal a deposition time-dependent crystallographic maturation that is crucial for tailoring ZnO nanostructures for optoelectronic and sensing applications [34].

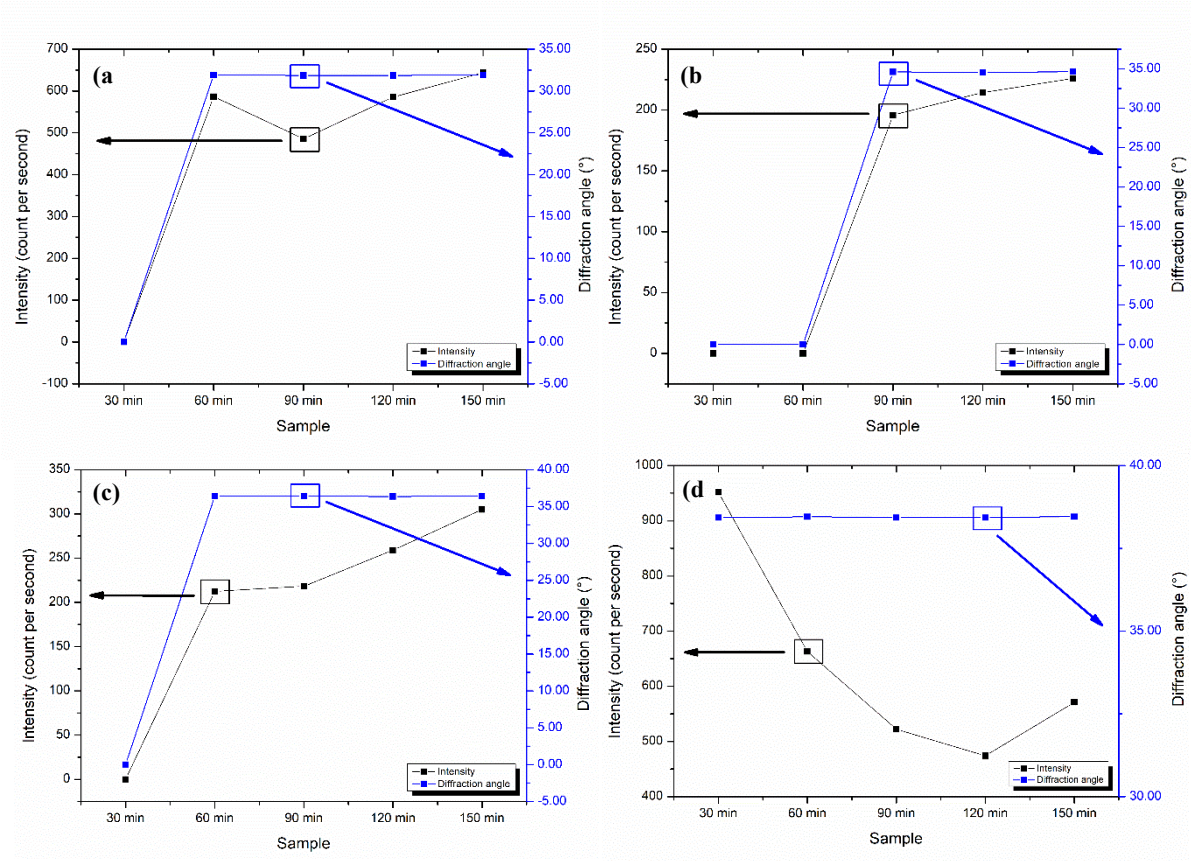

Figure 3. The intensities and diffraction angles of zinc oxide nanostructures prepared at various growth times a) peak (100) b) peak (002) c) peak (101) and d) peak (200)

Figure 4 show the surface morphology of ZnO-Ns using field emission scanning electron microscopy (FESEM) for various growth time from 30 min to 150 min. The sample with 30 min deposition time shows nanoflakes structures and at 120 min deposition time, it can be observed that nanorods structures started to develop up until 150 min. These FESEM images are correlated with XRD patterns as the sample of 30 min deposition time resulted in nanoflakes with cubic crystal structure of an average of crystallite size of 51.64 nm, the highest among all samples, compared with

the nanorods obtained of an average of crystallite size of 34.89 nm after 120 min of deposition time as shown in Figure 4 (d) due to the co-exist of both cubic and hexagonal structures. The evolution in morphology and density is closely linked to deposition time, short times yield limited nucleation sites and poor surface coverage, while longer times favour vertical growth and higher packing density. These morphological transitions also correlate with XRD-derived crystallite size and phase evolution. At 30 min, high average crystallite size (~51 nm) and nanoflakes morphology reflect the dominance of the cubic ZnO phase and sparse nucleation. By 120 min, when hybrid cubic–hexagonal phases coexist, denser, vertically oriented nanorods emerge and crystallite size decreases (~34.9 nm), reflecting high nucleation density and (002) orientation. At 150 min, the morphology stabilises into well-aligned rods with slightly lower density, consistent with structural maturity and possible supply-limited growth.

The observed morphology evolution confirms that deposition time is a critical parameter for optimising nanostructure uniformity, density and orientation. Control over these features is essential for applications requiring high surface area and consistent coverage, such as in sensors, piezoelectric devices and photocatalysis [35]. All images in figure 4 portrays that the growth time is a vital parameter in obtaining the morphology (density, size, shape, distribution, orientation and alignment) of the zinc oxide nanostructures [36].

The morphological structure of ZnO nanostructures significantly influences their optical properties, particularly transmittance. Surface morphology affects parameters such as roughness, grain boundary density and light-scattering behaviour. For example, planar or flake-like structures such as figure 4 (a) typically exhibit higher optical transmittance due to smoother surfaces and reduced light scattering, while vertically aligned or densely packed nanostructures such as figure 4 (d) tend to reduce transmittance due to enhanced light trapping and internal reflections. Morphology can also influence the optical band gap through quantum confinement effects or defect-related states, which alter the absorption edge and photoluminescence response [37]. As such, tailoring the morphology is essential for optimising the optical performance of ZnO films for applications like UV detectors, transparent electronics and optoelectronic devices [38].

Deposition time plays a critical role in determining the evolution of ZnO morphology. At shorter deposition times, such as 30 minutes, the growth is dominated by nucleation, resulting in smaller crystallites or thin, uniform layers with preferred orientations. With increasing deposition time, the nanostructures undergo morphological transitions due to extended crystal growth and particle aggregation, often forming larger, denser or more vertically aligned features. These structural changes not only affect the physical appearance but also impact film thickness, uniformity, and surface coverage, all of which directly influence the optical behaviour. Therefore, careful optimisation of deposition time is necessary to control the morphological development and achieve desirable optical and structural characteristics for specific device applications.

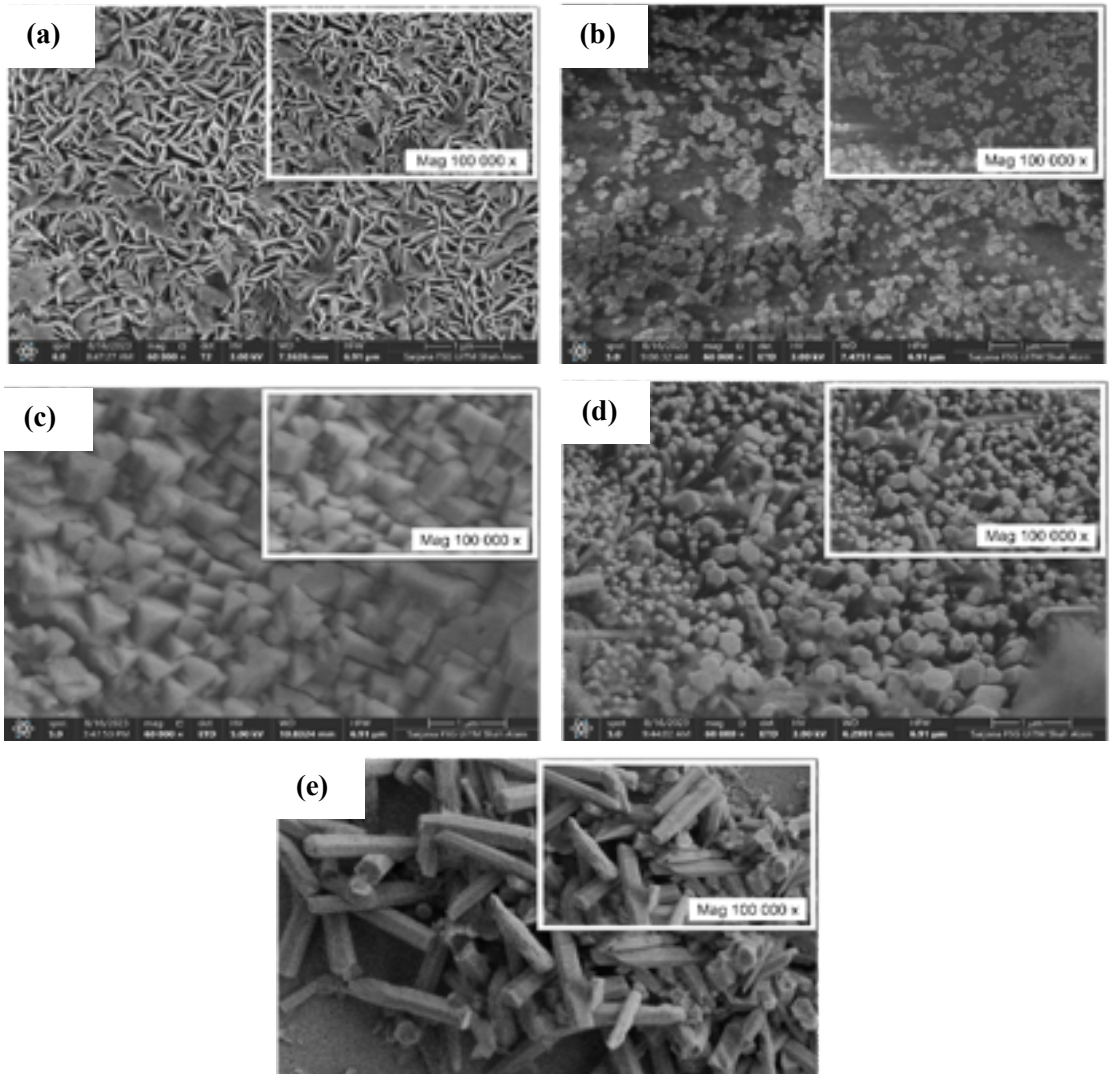

Figure 4. FESEM images of zinc oxide nanostructures grown at various growth time a) 30 b) 60 c) 90 d) 120 and e) 150 min.

Figure 5 exhibits the transmittance spectra of ZnO-Ns with varied deposition times. The average transmittances at the visible region are approximately 83.86%, 72.69%, 60.83%, 49.44%, and 36.23% for 30, 60, 90, 120 and 150 minutes, respectively. The transmittance percentage dropped as the deposition time rises. This reduction in optical transmittance with increasing deposition time is attributed to enhanced light scattering caused by increased grain boundary density and surface roughness [39]. Furthermore, the greater film thickness achieved with longer growth times enhances optical scattering, subsequently diminishing the transmittance of the thin films [40]. At 30 minutes, the high transmittance (~84%) reflects minimal film thickness, low surface rugosity and predominance of thin, lightly crystalline structures. As deposition proceeds to 60 minutes, a modest decrease to ~73% indicates onset of grain growth and roughening, increasing optical scattering at grain boundaries. By 90 minutes, the transmittance drops further to ~61%, evidencing thicker films and larger grain structures that reduce transparency due to enhanced scattering and possible defect absorption. At 120 minutes, transmittance falls sharply to ~49%, concurrent with dense nanorod formation and pronounced c-axis orientation visualized in FESEM and supported by XRD data. The increased grain boundary area and structural heterogeneity scatter transmitted light more effectively. At 150 minutes, the transmittance reaches ~36%, representing nearly opaque behaviour

in visible light, attributable to maximum thickness and high density of crystallites and surface irregularities.

Past studies confirm that increased film thickness elevates grain boundary scattering, thereby reducing optical transparency [41]. Moreover, thicker ZnO films or nanostructures assemblies exhibit additional absorption due to defect states and increased light path through the material. Surface roughness, defect density and structural disorder also contribute to lower transmittance in nanostructured ZnO films. Therefore, the measured transmittance values over time not only reflect morphological and structural evolution, but also have significant implications for the functional applications of ZnO in transparent electronics, sensors and photonic devices. To sum up, in this paper, the reduction in transmittance observed in the zinc oxide nanostructures, with increasing deposition time, can be attributed to two key factors. Firstly, the increase in film thickness over time led to the development of larger grain structures and an augmented surface roughness. Secondly, the heightened thickness of the zinc oxide nanostructures might contribute to a rise in absorption capacity.

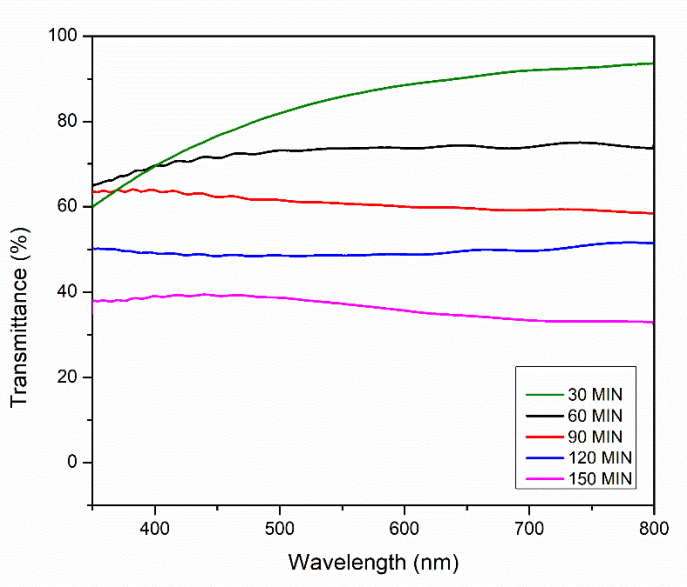

Figure 5. Transmission spectrum of zinc oxide nanostructures for different deposition time.

Figure 6 presents the time-dependent output voltage of the ZnO nanogenerator fabricated using nanostructures synthesised at a deposition time of 30 minutes, under periodic mechanical actuation. The output signal shows repetitive voltage peaks with a maximum amplitude reaching approximately 8 V, signifying robust piezoelectric behaviour of the ZnO nanostructures. The pronounced and consistent voltage spikes across the 6-second interval highlight the high responsiveness and stability of the device [42]. The selection of the 30-minute deposition time for testing is deliberate, as prior structural and morphological evaluations for XRD and FESEM confirmed this duration as the optimum condition yielding highly crystalline and uniform surface coverage. These characteristics are crucial for enhancing piezoelectric performance, as uniform nanostructures maximize the charge generation. The smoother and more uniform surface morphology achieved at 30 minutes promotes effective mechanical-to-electrical energy conversion, as deformation is more evenly distributed across the active layer. It is also notable that only the optimised ZnO sample (30-

minute deposition) was subjected to nanogenerator testing, as the study primarily aimed to assess its potential for real-world applications such as wearable or low-power environmental sensors. This approach aligns with industry-relevant material screening, where only the most promising synthesis conditions are scaled or integrated into device-level testing. Overall, the results validate that microwave-assisted sonochemical synthesis at the optimal deposition time can yield ZnO nanostructures capable of generating high piezoelectric voltage under ambient conditions. The ~8 V peak output affirms its potential as an energy harvesting material for next-generation flexible electronics and self-powered sensor platforms.

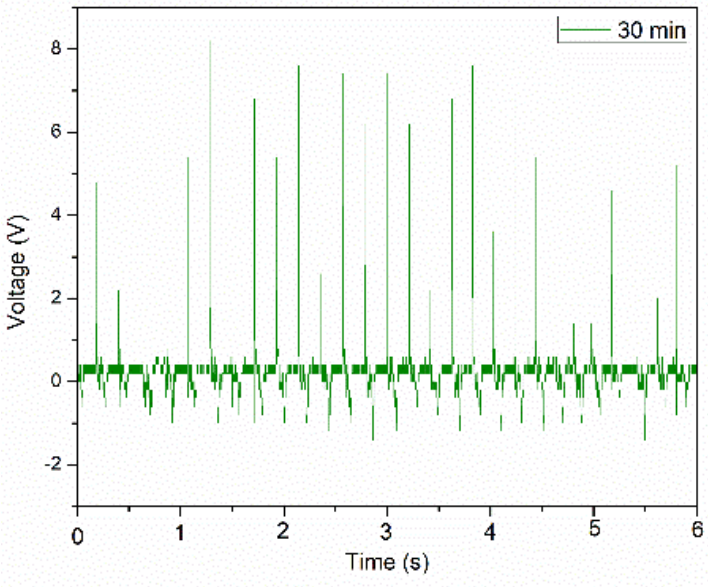

Figure 6. Output voltage measured using oscilloscope for ZnO nanogenerator.

4. Conclusion

In conclusion, the impact of deposition time on the synthesisation of zinc oxide-based nanostructures employing the microwave-assisted sonochemical technique had been proved to be a crucial parameter to be studied and further explore. It is observed that as the deposition time increased, the structural, morphological and optical properties of zinc oxide nanostructures also underwent evolution and changes. XRD patterns and FESEM images had been done and the co-existing of both cubic and hexagonal crystal structures were proven to be possible. Four peaks of zinc oxide and one PET peak were observed in the XRD data. The evolution of nanoflakes structures to nanorods structures is an evidence of how the deposition time could really affect the morphological properties of zinc oxide nanostructures. Additionally, UV-Vis analysis explained that the increase in film thickness over time might led to development of larger grain structures and an increment in absorption capacity. Lastly, the 30-minute sample, which is the optimum sample, was fabricated into a nanogenerator and the results of the output voltage was very promising which is near 8V. In conclusion, our comprehensive investigation into the influence of deposition time on zinc oxide-based nanostructures had contributed valuable knowledge to the field of nanomaterials synthesis and design. Our findings might serve as a guide for optimising the microwave-assisted sonochemical technique and tailoring zinc oxide nanostructures for specific applications in the future.

Acknowledgement

This work was supported in part by grant nos. 600-RMC/GPM CoE 5/3 (106/2022) and 600-RMC/GIP 5/3 (098/2021). The authors would like to thank the Research Management Centre of the Universiti Teknologi MARA (UiTM) and Ministry of Higher Education (MoHE), Malaysia for financial support. The authors also thank Mr. Salifairus Mohammad Jafar (UiTM Senior Science Officer), Mr. Mohd Azlan Jaafar (UiTM assistant engineer), Mr. Suhaimi Ahmad (UiTM assistant engineer) and Mr. Muhamad Faizal Abd Halim (Assistant Research Officer) for their kind support on this research.

References

[1] Asif, Muhammad H., Aamir Razaq, Sunil Bhand, Magnus Willander, and Bengt Danielsson. "Chapter 2 - Biosensors for Intracellular and Less Invasive Measurements Based on Nanostructured Metal Oxides." In *Nanotechnology and Biosensors*, edited by Dimitrios P. Nikolelis and Georgia-Paraskevi Nikoleli, 29-49: Elsevier, 2018.

[2] Verma, Ketki, Dhiraj Kumar Bharti, Simadri Badatya, Avanish Kumar Srivastava, and Manoj Kumar Gupta. "A High Performance Flexible Two Dimensional Vertically Aligned Zno Nanodisc Based Piezoelectric Nanogenerator Via Surface Passivation." *Nanoscale Advances* 2, no. 5 (2020-01-01 2020): 2044-51. https://doi.org/10.1039/c9na00789j.

[3] Lee, Yoonjung, Sohee Kim, Daeyeong Kim, Cheoljae Lee, Hyojin Park, and Ju-Hyuck Lee. "Direct-Current Flexible Piezoelectric Nanogenerators Based on Two-Dimensional Zno Nanosheet." *Applied Surface Science* 509 (2020/04/15/ 2020): 145328. https://doi.org/https://doi.org/10.1016/j.apsusc.2020.145328.

[4] Chu, Y. L., S. J. Young, L. W. Ji, T. T. Chu, and P. H. Chen. "Synthesis of Ni-Doped Zno Nanorod Arrays by Chemical Bath Deposition and Their Application to Nanogenerators." *Energies* 13, no. 11 (Jun 2020): 2731. https://doi.org/10.3390/en13112731.

[5] Wang, Chao-Nan, Yu-Liang Li, Fei-Long Gong, Yong-Hui Zhang, Shao-Ming Fang, and Hao-Li Zhang. "Advances in Doped Zno Nanostructures for Gas Sensor." *The Chemical Record* 20, no. 12 (2020): 1553-67.

[6] Taşdemir, Abdulkadir, Nazife Akman, Abdullah Akkaya, Raşit Aydın, and Bünyamin Şahin. "Green and Cost-Effective Synthesis of Zinc Oxide Thin Films by L-Ascorbic Acid (Aa) and Their Potential for Electronics and Antibacterial Applications." *Ceramics International* 48, no. 7 (2022/04/01/ 2022): 10164-73. https://doi.org/https://doi.org/10.1016/j.ceramint.2021.12.228.

[7] Yuan, Ming, Ruixue Ma, Qiuyang Ye, Xue Bai, Hanchuan Li, Feifei Yan, Chuntai Liu, Yue Ren, and Zhen Wang. "Melt-Stretched Poly(Vinylidene Fluoride)/Zinc Oxide Nanocomposite Films with Enhanced Piezoelectricity by Stress Concentrations in Piezoelectric Domains for Wearable Electronics." *Chemical Engineering Journal* 455 (2023/01/01/ 2023): 140771. https://doi.org/https://doi.org/10.1016/j.cej.2022.140771.

[8] Nava, O., F. N. Murrieta-Rico, M. E. Martínez-Rosas, M. J. Chinchillas-Chinchillas, H. E. Garrafa-Galvez, A. R. Vilchis-Nestor, and P. A. Luque. "Evaluation of Electrochemical Properties of Zinc Oxide Based Semiconductor Nanoparticles Biosynthesized with Mentha Spicata for Optoelectronic Applications." *Materials Letters* 275 (2020/09/15/ 2020): 128101. https://doi.org/https://doi.org/10.1016/j.matlet.2020.128101.

[9] Morales–Morales, F., A. Benítez-Lara, N. Hernández-Sebastián, F. Ambriz-Vargas, M. R. Jiménez-Vivanco, R. López, and A. Morales–Sánchez. "Study of Zinc Oxide/Porous Silicon Interface for Optoelectronic Devices." *Materials Science in Semiconductor Processing* 148 (2022/09/01/ 2022): 106810. https://doi.org/https://doi.org/10.1016/j.mssp.2022.106810.

[10] Kanakkillam, Sreed S., S. Shaji, B. Krishnan, S. Vazquez-Rodriguez, J. A. Aguilar Martinez, M. I. Mendivil Palma, and D. A. Avellaneda. "Nanoflakes of Zinc Oxide:Cobalt Oxide Composites by Pulsed Laser Fragmentation for Visible Light Photocatalysis." *Applied Surface Science* 501 (2020/01/31/ 2020): 144223. https://doi.org/https://doi.org/10.1016/j.apsusc.2019.144223.

[11] Atta-Eyison, Aba Akebi, Gloria Daisy Anukwah, and Ruphino Zugle. "Photocatalysis Using Zinc Oxide-Zinc Phthalocyanine Composite for Effective Mineralization of Organic Pollutants." *Catalysis Communications* 160 (2021/12/01/ 2021): 106357. https://doi.org/https://doi.org/10.1016/j.catcom.2021.106357.

[12] Hartini Ahmad Rafaie, Zul Adlan Mohd Hir, Nurul Infaza Talalah Ramli and Muhd Firdaus Kasim. "Synthesis, Characterization and Photocatalytic Activities of Mg-Doped Zno for Degradation of Methylene Blue Dye under Uv Light Irradiation." *Malaysian Journal of Analytical Sciences* 27, no. 2 (2023): 304-13.

[13] Mohammad, Mahaboob Jahanara, A. Sudha, Manasa Hari Adavalli, and Parasuraman Swaminathan. "Room Temperature Chemiresistive Sensing of Carbon Dioxide Using a Composite of Zinc Oxide and Nickel Oxide."

Surfaces and Interfaces 41 (2023/10/01/ 2023): 103155. https://doi.org/https://doi.org/10.1016/j.surfin.2023.103155.

[14] Rudra, Pratyasha, Nirman Chakraborty, Velaga Srihari, Ajay K. Mishra, Sagnik Das, Debdulal Saha, and Swastik Mondal. "Effect of Dopant Oxidation States on Enhanced Low Ppm Co Sensing by Copper Doped Zinc Oxide." *Materials Chemistry and Physics* 295 (2023/02/01/ 2023): 127047. https://doi.org/https://doi.org/10.1016/j.matchemphys.2022.127047.

[15] Kamaruzaman, Dayana, Mohamad Hafiz Mamat, Nurul Izzati Kamal Ariffin, A Shamsul Rahimi A Subki, Mohd Hanapiah Abdullah, Norfarariyanti Parimon, Muhamad Kamil Yaakob*, et al.* "Effects of Thermal Annealing on the Morphology and Structural Characteristics of Zinc Oxide Nanopowders for Triboelectric Nanogenerator Applications." *Journal of Advanced Research in Fluid Mechanics and Thermal Sciences* 99, no. 1 (2022-10-17 2022): 17-27. https://doi.org/10.37934/arfmts.99.1.1727.

[16] Jaffri, S., K. Ahmad, Isaac Abrahams, and Adel El-Marghany. "Microwave Fostered Sustainable Synthesis of Nb2o5 – Zno Nanomaterial for Efficiency Amplification in High Performing Energy Systems." *Optical Materials* (2024-10-01 2024). https://doi.org/10.1016/j.optmat.2024.116304

[17] Kumar, Anuj, Yun Kuang, Zheng Liang, and Xiaoming Sun. "Microwave Chemistry, Recent Advancements, and Eco-Friendly Microwave-Assisted Synthesis of Nanoarchitectures and Their Applications: A Review." *Materials Today Nano* 11 (2020/08/01/ 2020): 100076. https://doi.org/https://doi.org/10.1016/j.mtnano.2020.100076.

[18] Abdulrahman, Ahmed, Sabah Ahmed Al-Jeboori, and Munirah Almessiere. "Effect of the Growth Time on the Optical Properties of Zno Nanorods Grown by Low Temperature Method." *Digest Journal of Nanomaterials and Biostructures* 12 (10/01 2017): 1001-09.

[19] Dloo, A., N. Fazouan, and E. H. Atmani. "Investigation of Hydrothermal Growth Time and Temperature for Optimized Zno Nanowire Arrays toward Photovoltaics." *Surfaces and Interfaces* 40 (2023/08/01/ 2023): 103123. https://doi.org/https://doi.org/10.1016/j.surfin.2023.103123

[20] Viju, Kumar V. G., P. Sreeshma, and V. G. Vidya. "Synthesis and Characterization of Cobalt- Zinc Oxide Nanoparticles Via Microwave Assisted Polyol Method." *Research Journal of Chemistry and Environment* (2023-09-15 2023). https://doi.org/10.25303/2710rjce021026.

[21] Tiss, B., D. Martínez-Martínez, B. Silva, N. Bouguila, El Mir, B. Almeida, C. Moura, and L. Cunha. "Growth of Al:Zno Nano-Flowers by Pulsed Laser Ablation Deposition." *Optics & Laser Technology* (2024-02-07 2024). https://doi.org/10.1016/j.optlastec.2024.110673.

[22] Li, Chaoyang. "Crystallinity-Driven Formation of Highly Arrayed Zno Nanorods Via Low-Temperature Chemical Bath Deposition on Transparent Conductive Oxide Substrates." *ECS Meeting Abstracts* (2024-08-09 2024). https://doi.org/10.1149/ma2024-01321581mtgabs.

[23] Malek, Mohd Firdaus, Mohamad Hafiz Mamat, Mohd Zainizan Sahdan, Musa Mohamed Zahidi, Zuraida Khusaimi, and Mohamad Rusop Mahmood. "Influence of Various Sol Concentrations on Stress/Strain and Properties of Zno Thin Films Synthesised by Sol–Gel Technique." *Thin Solid Films* 527 (2013/01/01/ 2013): 102-09. https://doi.org/https://doi.org/10.1016/j.tsf.2012.11.095.

[24] Muthukumar, Harshiny, Ashish Gire, Meena Kumari, and Matheswaran Manickam. "Biogenic Synthesis of Nano-Biomaterial for Toxic Naphthalene Photocatalytic Degradation Optimization and Kinetics Studies." *International Biodeterioration & Biodegradation* 119 (2017/04/01/ 2017): 587-94. https://doi.org/https://doi.org/10.1016/j.ibiod.2016.10.036.

[25] Nezamabadi, Vida, M. Akhgar, Batool Tahamipour, and Peyman Rajaei. "Biosynthesis and Antibacterial Activity of Zno Nanoparticles by Artemisia Aucheri Extract." *Iranian journal of biotechnology* 18 (04/01 2020): e2426. https://doi.org/10.30498/IJB.2020.151379.2426.

[26] Nasrin, Rahima, M. Haq, Md Mohiuddin, and H. Akther. "Effect of Deposition Parameter on Exterior Morphology, Structural and Optical Characteristics of Chemical Bath Deposited Zinc Oxide Thin Films." *Surface Review and Letters* (2023-11-24 2023). https://doi.org/10.1142/s0218625x24500598.

[27] Strachowski, T., M. Baran, Marc Malek, R. Kosturek, E. Grzanka, J. Mizeracki, Agata Romanowska, and Stefan Marynowicz. "Hydrothermal Synthesis of Zinc Oxide Nanoparticles Using Different Chemical Reaction Stimulation Methods and Their Influence on Process Kinetics." *Materials* 15 (2022-10-31 2022). https://doi.org/10.3390/ma15217661.

[28] Tran, Bao Quan, Hai Dang Ngo, and Thi Kim Hang Pham. "Influence of Growth Temperature on Morphological and Structural Properties of Sputtered- Zinc Oxide Nanorods." *Journal of Technical Education Science* (2024-08-28 2024). https://doi.org/10.54644/jte.2024.1404.

[29] Zhang, Binbin, Wenhui Zhang, Wei Luo, Zhijie Liang, Yan Hong, Jianhui Li, Guoyun Zhou, and Wei He. "Morphology-Dependent Behavior of Pvdf/Zno Composites: Their Fabrication and Application in Pressure Sensors." *Sensors (Basel, Switzerland)* 25 (2025-05-01 2025). https://doi.org/10.3390/s25092936.

[30] Cheng, Ya-Chih, Sanjaya Brahma, Sean Wu, Jow-Lay Huang, and Alex Lee. "Crystal Structure Evolution of Piezoelectric Fe-Doped Zno Film by Magnetron Co-Sputtering Technique." *Condensed Matter* (2025-01-15 2025). https://doi.org/10.3390/condmat10010006.

[31] Aadim, K., and I. Abbas. "Synthesis and Investigation of the Structural Characteristics of Zinc Oxide Nanoparticles Produced by an Atmospheric Plasma Jet." *Iraqi Journal of Science* (2023-04-30 2023). https://doi.org/10.24996/ijs.2023.64.4.15.

[32] Hathot, S., S. Abbas, H. A. T. AlOgaili, and A. Salim. "Influence of Deposition Time on Absorption and Electrical Characteristics of Zns Thin Films." *Optik* (2022-04-01 2022). https://doi.org/10.1016/j.ijleo.2022.169056.

[33] Khan, H., Aditya Yerramilli, Adrien D'Oliveira, T. Alford, D. Boffito, and G. Patience. "Experimental Methods in Chemical Engineering: X-Ray Diffraction Spectroscopy— Xrd." *The Canadian Journal of Chemical Engineering* (2020-03-10 2020). https://doi.org/10.1002/cjce.23747.

[34] El-Khayatt, A., E. Abdel-Fattah, and A. Azab. "The Effect of Annealing Temperature on the Structural, Optical, and Magnetic Properties of Zno@ Nife2o4 Nanocomposites." *Physica Scripta* 100 (2025-04-11 2025). https://doi.org/10.1088/1402-4896/adcbe6.

[35] A. F. ABDULRAHMAN, S. M. AHMED, M. A. ALMESSIERE. "Effect of the Growth Time on the Optical Properties of Zno Nanorods Grown by Low Temperature Method." *Digest Journal of Nanomaterials and Biostructures* 12, no. No. 4, October-December 2017 (2017): 1001-09.

[36] Abdulrahman, Ahmed F., Sabah M. Ahmed, and Naser M. Ahmed. "Investigation of Optical Properties of Zno Nanorods Grown on Different Substrates." *Science Journal of University of Zakho* 6, no. 4 (2018-12-30 2018): 160-65. https://doi.org/10.25271/sjuoz.2018.6.4.546.

[37] Nadeem, M., Miao Baoji, Mohammed Mujahid Alam, Nagina Naveed Riaz, A. Al-Sehemi, Tauseef Munawar, Faisal Mukhtar*, et al.* "Sr-Doped Zno Thin Film on a Silicon Substrate (100) Grown by Sol-Gel Method: Structural and Optical Study." *Optical Materials* (2024-09-01 2024). https://doi.org/10.1016/j.optmat.2024.116106.

[38] Wang, Li-Yuan, Bing-Yin Shi, Chenguang Yao, Ze Wang, Xue Wang, C. Jiang, Li Feng, and Yingru Song. "Size and Morphology Modulation in Zno Nanostructures for Nonlinear Optical Applications: A Review." *ACS Applied Nano Materials* (2023-06-09 2023). https://doi.org/10.1021/acsanm.3c01509.

[39] Mosalagae, K., D.M. Murape, and L.M. Lepodise. "Effects of Growth Conditions on Properties of Cbd Synthesized Zno Nanorods Grown on Ultrasonic Spray Pyrolysis Deposited Zno Seed Layers." *Heliyon* 6, no. 7 (2020-07-01 2020): e04458. https://doi.org/10.1016/j.heliyon.2020.e04458.

[40] Malek, Mohd Firdaus, Mohamad Hafiz Mamat, Tetsuo Soga, Saadah Abdul Rahman, Suriani Abu Bakar, Ahmad Syakirin Ismail, Ruziana Mohamed*, et al.* "Thickness-Controlled Synthesis of Vertically Aligned C-Axis Oriented Zno Nanorod Arrays: Effect of Growth Time Via Novel Dual Sonication Sol–Gel Process." *Japanese Journal of Applied Physics* 55, no. 1S (2015/12/14 2016): 01AE15. https://doi.org/10.7567/JJAP.55.01AE15.

[41] Hopoğlu, H., H. Aydınoğlu, A. Özer, and Şenadım Tüzemen. "Investigation of Nitrogen Doped Zno Thin Films: Effects on Their Structural and Optical Properties." *Optical Materials* (2021-12-01 2021). https://doi.org/10.1016/j.optmat.2021.111685.

[42] Kaur, J., and H. Singh. "Fabrication and Analysis of Piezoelectricity in 0d, 1d and 2d Zinc Oxide Nanostructures." *Ceramics International* 46 (2020-08-01 2020): 19401-07. https://doi.org/10.1016/j.ceramint.2020.04.283.